Calcif Tissue Int (1993) 53:348–356

Calcified
Tissue
International

Osteoclastic Resorption of Ca-P Biomaterials Implanted in Rabbit Bone

Michel F. Baslé,[1,2] Daniel Chappard,[1] Florence Grizon,[1] Robert Filmon,[2] Joël Delecrin,[3] Guy Daculsi,[3] and André Rebel[1]

[1]Laboratoire d'Histologie-Embryologie, Faculté de Médecine, rue Haute de Reculée, 49045 Angers-Cedex, France; [2]Service Commun de Microscopie Electronique, Université d'Angers, France; and [3]Laboratoire de Recherche sur les Tissus Calcifiés et les Biomatériaux, Faculté de Chirurgie Dentaire, Nantes, France

Received April 14, 1993, and in revised form June 14, 1993

Summary. The nature of the multinucleated cells involved in the resorption processes occurring inside macroporous calcium-phosphate biomaterials grafted into rabbit bone was studied using light microscopy, histomorphometric analysis, enzymatic detection of tartrate-resistant acid phosphatase (TRAP) activity, scanning, and electron microscopy. Samples were taken at days 7, 14, and 21 after implantation. As early as day 7, osteogenesis and resorption were observed at the surface of the biomaterials, inside the macropores. Resorption of both newly formed bone and calcium-phosphate biomaterials was associated with two types of multinucleated cells. Giant multinucleated cells were found only at the surface of the biomaterials; they showed a large number of nuclei, were TRAP negative, developed no ruffled border, and contained numerous vacuoles with large accumulation of mineral crystals from the biomaterials. Osteoclasts exhibited TRAP positivity and well-defined ruffled border. They were observed at the surface of both newly formed bone and biomaterials, around the implant, and inside the macropores. In contact with the biomaterials, infoldings of their ruffled border were observed between the mineral crystals, deeply inside the microporosity. The microporosity of the biomaterials (i.e., the noncrystalline spaces inside the biomaterials) increased underneath this type of cell as compared with underneath giant cells or to the depth of the biomaterials. These observations demonstrate that macroporous calcium-phosphate biomaterials implanted in bone elicit osteogenesis and the recruitment of a double multinucleated cell population having resorbing activity: giant multinucleated cells that resorb biomaterials and osteoclasts that resorb newly formed bone and biomaterials.

Key words: Osteoclast – Giant multinucleated cell – Biomaterials – Ceramics – Morphometry – Bone.

Various porous synthetic or natural calcium-phosphate (Ca-P) materials have been developed and used as bone substitute for clinical applications [1]. When grafted in a bone site, ingrowth of vascularized connective tissue into the macropores of the implant is followed by osteogenesis, with bone deposition at the surface of the biomaterial [2–4]. It was reported that such biomaterials cannot induce bone formation in heterotopic site, however, osteogenesis was observed in subcutaneous implant when the biomaterial was combined with bone marrow cells [5].

Resorption of the newly formed bone and of the Ca-P ceramics also occurs, and multinucleated cells are found in contact with the biomaterial. However, the nature and origin of these multinucleated cells remain incompletely elucidated and even conflicting. It was reported that the multinucleated cells elicited in contact with synthetic hydroxyapatite implanted in bone [6] or with mineralized bone particles subcutaneously implanted in rat [7] developed some morphological and functional features of osteoclast such as tartrate-resistant acid phosphatase (TRAP) activity and ruffled border with clear zones. In contrast, the multinucleated cells recruited in contact with hydroxyapatite implanted in human periodontium or in contact with mineralized bone particles subcutaneously implanted in rabbit, lack TRAP activity, cell surface aspects, and functional features of osteoclasts [8, 9]. So, the term "multinucleated cell" may be confusing as it often includes osteoclast and giant cell of the foreign body reaction.

Osteoclasts are the main cells involved in the resorption of mineralized bone tissue. They differentiate in contact with bone from mononucleated medullar precursors [10, 11], and a lot of systemic and local factors have demonstrated an effective influence on their differentiation [11–13]. However, morphological and histochemical features usually provide sufficient support for cell identification.

Giant multinucleated cells also termed "Langhans cells" or "foreign body giant cells," containing a large number of nuclei, have been described in chronic inflammatory tissue reaction (granuloma). They do not show a ruffled border or TRAP activity and they originate by fusion of mature monocytes or macrophages [14–17].

In the present study we have attempted to determine the nature of the cells involved in the resorption processes observed in such Ca-P ceramics, after implantation in corticomedullar defects drilled in tibiae of young rabbits. Two types of Ca-P biomaterials were used to test the specificity of the cellular and tissular reactions to implantation in bone. Histological and electron microscopic examination of resorbing cells were completed by histomorphometric analysis, histoenzymatic determination of the tartrate-resistant acid phosphatase activity, and measurement of the microporosity of the biomaterials.

Materials and Methods

Two types of cylindrical Ca-P ceramic (60 samples), 4 mm in length

Offprint requests to: M. F. Baslé at the Laboratoire d'Histologie-Embryologie

and 2.5 mm in diameter, were implanted in 15 young adult New Zealand white rabbits, each of them receiving two implants in the left tibiae and two implants in the right (one type of ceramic by tibia): (1) macroporous biphasic calcium phosphate (MBCP, 30 implants) consists of a 60/40 mixture (weight ratio) of synthetic hydroxyapatite $Ca_{10}(PO_4)_6(OH)_2$ and β tricalcium phosphate $(Ca_3(PO_4)_2$ compacted and sintered, at 1100°C, in macroporous blocks (40–50% macroporous, macropores from 400 to 600 μm in diameter); (2) bovine hydroxyapatite (Bonap, 30 implants), a bovine bone hydroxyapatite, was prepared by deproteinization of trabecular bovine bone and hydrothermal transformation of the inorganic phase into hydroxyapatite (this biomaterial was a gift from Dr. R. Legeros, College of Dentistry, New York University).

Implantations were performed, under sterile conditions and general anesthesia, in tibial cortico-medullar defects drilled at low speed under sterilized saline coolant, at about 15 mm from the proximal metaphyseal plate. Biopsies containing the implants were harvested 3, 7, 14, and 21 days after implantation.

Histological studies were carried out on 48 samples (24 MBCP, 24 Bonap), 4% paraformaldehyde-fixed, 7.5% buffered-EDTA decalcified, and paraffin embedded. The 7-μm sections were used for histological observation, histomorphometric analysis, and TRAP detection.

Light microscopic observations were done on sections stained with hematoxylin and eosine (H & E) and Masson's trichrome, using a photomicroscope Nikon UFX II.

Histomorphometric measurements of the implants were carried out using a Zeiss microscope equipped with an integratory 100-points eyepiece reticule. The following measurements were carried out and expressed according to the ASBMR Histomorphometry Nomenclature Committee, using implant volume (Imp.V) as referent: biomaterial volume (Bm.V/Imp.V) and thickness of trabeculae (Bm.Th.) of the biomaterials, and volume of the newly formed bone (NFB.V/Imp.V). These measurements were performed, before implantation (day 0), on undecalcified and methylmethacrylate-embedded specimens, because decalcification of the nonimplanted samples led to the dissolution of the biomaterials.

TRAP activity was identified using naphtol AS BI phosphate (Sigma) as substrate with freshly diazotized Fast Garnet GBC (Sigma), in the presence of 50 mM tartrate. The number of multinucleated cells, either TRAP+ or TRAP−, in contact with newly formed bone or with biomaterials, was determined and expressed per mm^2 of the implant area (Imp.Ar.).

Electron microscopic observation was done on biomaterials before implantation and on samples, taken at days 7, 14, and 21. Specimens were fixed for 90 mn, at +4°C, in a 4.5% glutaraldehyde solution in pH 7.4 phosphate saline buffer and washed in phosphate buffer. These specimens were then processed for either transmission electron microscopy (TEM) or scanning electron microscopy (SEM).

SEM examination was done by two sequential methods: (1) after fixation and rinsing, fragments were dehydrated in a series of graded ethanol and acetone, critical-point dried, gold coated, and examined in a Jeol JSM 35 SEM; (2) after observation, fragments were rehydrated in distilled water, placed in a 10% sodium hypochlorite aqueous solution for about 6 hours, washed in distilled water, dehydrated, and then processed as above; this treatment removes the organic fraction. The same procedure was applied to two nonimplanted samples to serve as controls and to six implanted samples (3 MBCP and 3 Bonap).

TEM observation was carried out on two nonimplanted specimens used as controls and on six implanted samples (3 MBCP, 3 Bonap), broken up into fragments about 1 mm^3 and separately embedded, undecalcified, in 812 resin epoxy. Multiple semiserial, ultrathin sections, 40–60 nm thick, were obtained using a diamond knife, stained with uranyl acetate and lead citrate, and observed using a 100 C Jeol electron microscope. The microporosity was calculated for each biomaterial, before implantation and on samples taken at day 14. Microporosity expressed the percentage of the surface area of the biomaterial not occupied by the mineral crystals. Image analysis was performed, on photographs (A4 format) at the original magnification of ×5000, using a point-counting method. Measurements were done in the region underneath multinucleated cells and in the depth of the biomaterial.

All values are expressed using mean ± SD. Comparisons between groups were done with Student's t test.

Results

Light microscopic examination of samples at day 3 after implantation showed loose connective tissue inside the superficial macropores of both biomaterials. Neither bone formation nor multinucleated cells were found in contact with the surface of the biomaterials. Histomorphometric analysis showed no significant variation in Bm.V/Imp.V or Bm.Th. when compared with preimplantation condition (results not shown).

From day 7 after implantation, seams and trabeculae made of newly formed bone, covered by layers of plump osteoblasts, were observed in the macropores, bound to the surface of the biomaterials in both types of implants (Fig. 1). Multinucleated cells were present as early as day 7, at the surface of both newly formed bone and biomaterials.

Most of the resorption cell profiles contained 2–10 nuclei; TRAP+ activity was detected in these cells and in the underlying biomaterial (Fig. 2). These cells, observed at the surface of the newly formed bone (NFB) and of the biomaterials, were similar to host osteoclasts found in the bone tissue distant from the implant or in the metaphyseal growth plates, and were designated as osteoclast-like cells (OLC). Some giant multinucleated cells (GMNC), containing more than 20 nuclei and showing no TRAP activity, were observed but only at the surface of the biomaterials (Fig. 3).

Histomorphometric analysis showed, before implantation, that in MBCP, (n = 4), Bm.V/Imp.V = 49.6 ± 4.1%, Bm.Th. = 345 ± 61 μm; in Bonap, (n = 4), Bm.V/Imp.V = 48.1 ± 3.2%, Bm.Th. = 295 ± 35 μm). After implantation, Bm.V/Imp.V progressively decreased in both biomaterials, whereas newly formed bone NFB.V/Imp.V increased (Fig. 4). In Bonap, Bm.Th. decreased to 163 ± 25 μm at day 21 after implantation ($P < 0.001$). Because of the partial dissolution of MBCP, occurring during the histological procedures, trabecular thickness could not be calculated for this biomaterial.

The total number of TRAP+ multinucleated cells (OLC_{Total}/Imp.Ar.) progressively increased in both implants. The number of OLC in contact with the biomaterials (OLC_{Bm}/Bm.Ar.) or with the newly formed bone (OLC_{NFB}/NFB.Ar.) increased in MBCP from day 7 to day 14, was similar at day 14 and day 21, and, in Bonap, increased progressively from day 7 to day 21. In both biomaterials, the number of GMNC (GMNC/Imp.Ar.; GMNC/Bm.Ar.) increased from day 7 to day 14 and decreased from day 14 to day 21 (Fig. 5).

Scanning electron microscopic observation showed, from day 7 after implantation, numerous cells, some reaching 100 μm in length, lying at the surface of the biomaterials in the macropores (Fig. 6). After treatment with sodium hypochlorite, new bone tissue was observed in the form of layers or trabeculae bound to the surface of the biomaterials (Fig. 7). Large zones of resorption with multiple pits were observed at the surface of the newly formed bone, and small pits 10–20 μm in diameter were also found at the biomaterial surfaces (Fig. 8).

Transmission electron microscopic study showed that the giant multinucleated cells in contact with the biomaterials contained numerous vacuoles in which a large accumulation of mineral crystals was observed (Fig. 9). No ruffled border was observed in this type of giant cells on the multiple ultrathin sections. A ruffled border, with clear zones, was found in smaller multinucleated cells in contact with the biomaterials (Fig. 10). Infoldings of the ruffled border were found inside the biomaterial itself, in the spaces left between the mineral crystals (Fig. 11). In these cells, nuclei were irregularly shaped, mitochondria were numerous, and no or few vacuoles containing mineral crystals were present. A

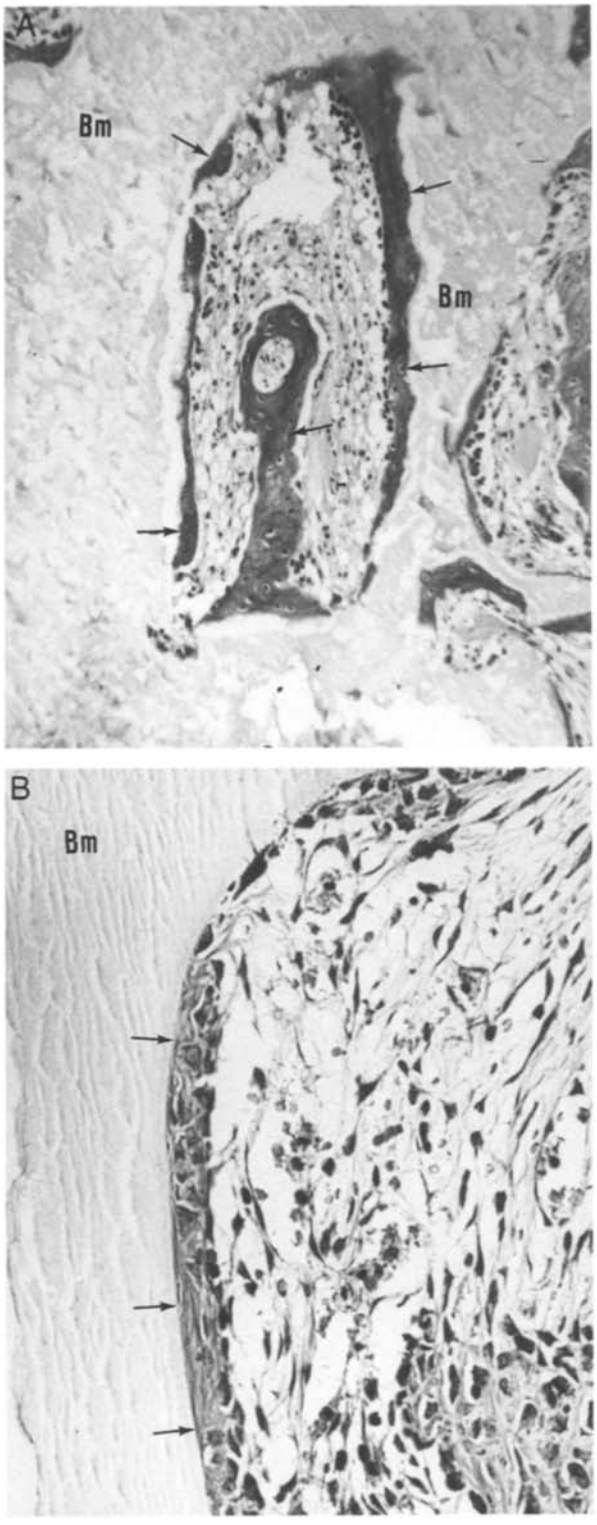

Fig. 1. Light microscopy of samples taken at day 7 after implantation. Newly formed bone is visible (→) at the surface of the macropores, inside the biomaterial (Bm): (A) MBCP (×70) and (B) Bonap (×250). Masson's Trichrome.

well-defined ruffled border was also observed in osteoclasts resorbing newly formed bone (Fig. 12).

After implantation, the microporosity of the ceramics increased underneath OLC in both biomaterials, compared with before implantation, to the region underneath GMNC

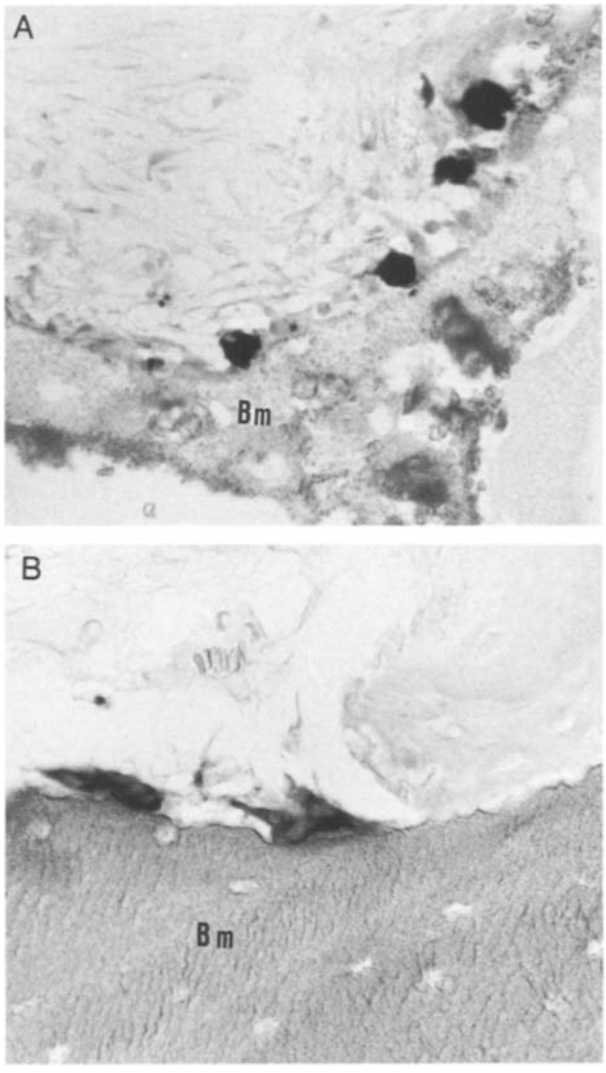

Fig. 2. Enzymatic detection at day 14 of the TRAP in osteoclast-like cells at the surface of (A) MBCP Bm (×200) and (B) Bonap biomaterial (×250).

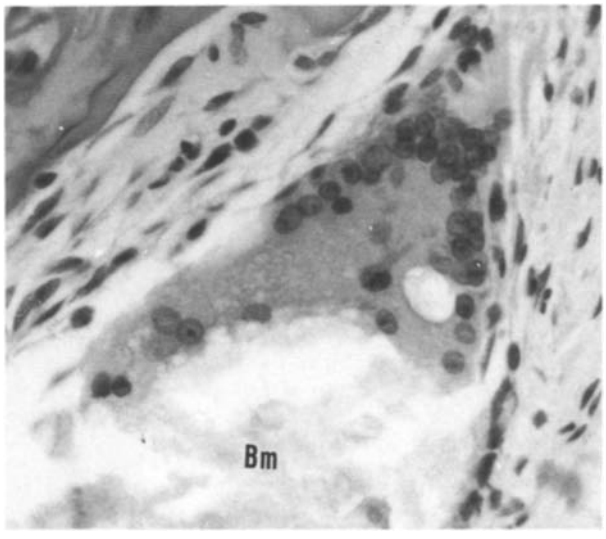

Fig. 3. Light microscopy at day 14 of giant multinucleated cell in contact with MBCP Bm. Note the semicircular disposition of nuclei (×400) H & E.

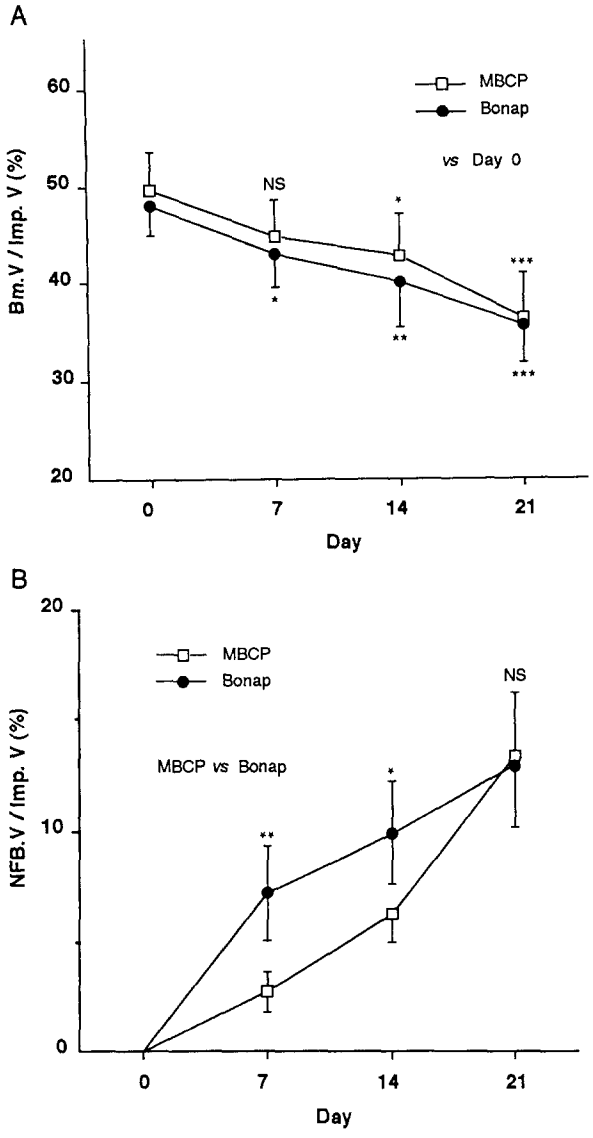

Fig. 4. Histomorphometric evolution after implantation of (**A**) volume of biomaterials (Bm.V/Imp.V), and (**B**) volume of newly formed bone (NFB.V/Imp.V) in MBCP and Bonap (NS = nonsignificant difference. $*P < 0.05$, $**P < 0.01$, $***P < 0.001$).

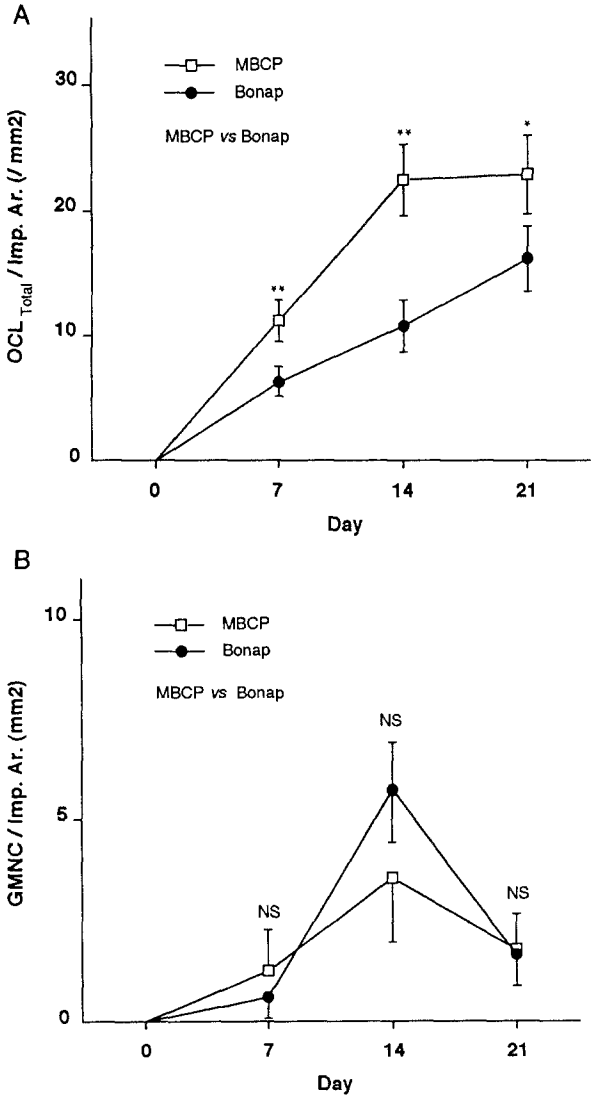

Fig. 5. Histomorphometric evolution after implantation of (**A**) number of osteoclast-like cells (OCL_{Total}/Imp.Ar.) and (**B**) giant multinucleated cells (GMNC/Imp.Ar.) in MBCP and Bonap implants. (NS: nonsignificant difference, $*P < 0.05$, $**P < 0.01$.)

or to the depth of the trabeculae. In Bonap, the microporosity was 56.0 ± 4.6% before implantation and increased at day 14 up to 77.2 ± 4.8% underneath OLC, but it remained at 61.7 ± 4.5% underneath GMNC and 60.8 ± 3.9% in the depth of the trabeculae. In MBCP, the microporosity was 54.1 ± 3.7% before implantation and increased at day 14 up to 70.7 ± 5.2% underneath OLC. Microporosity remained at 59.8 ± 4.9% underneath GMNC and 58.7 ± 4.1% in the depth (Fig. 13).

Discussion

Osteoclasts are the major cells responsible for the physiological resorption of mineralized bone [11, 12, 18]. These cells show morphological and functional characteristics: they are multinucleated, they develop a typical ruffled border in contact with mineralized bone matrix [11, 19, 20], they are capable of acidifying the extracellular compartment leading to extracellular dissolution of the Ca-P crystals [21–23], they show TRAP and ATPase activity [24, 25] although the

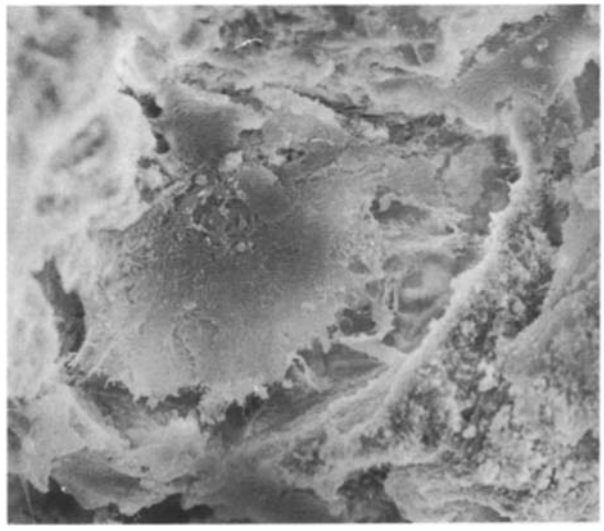

Fig. 6. SEM at day 14 of a large cell in resorption lacunae at the surface of MBCP Bm (×280).

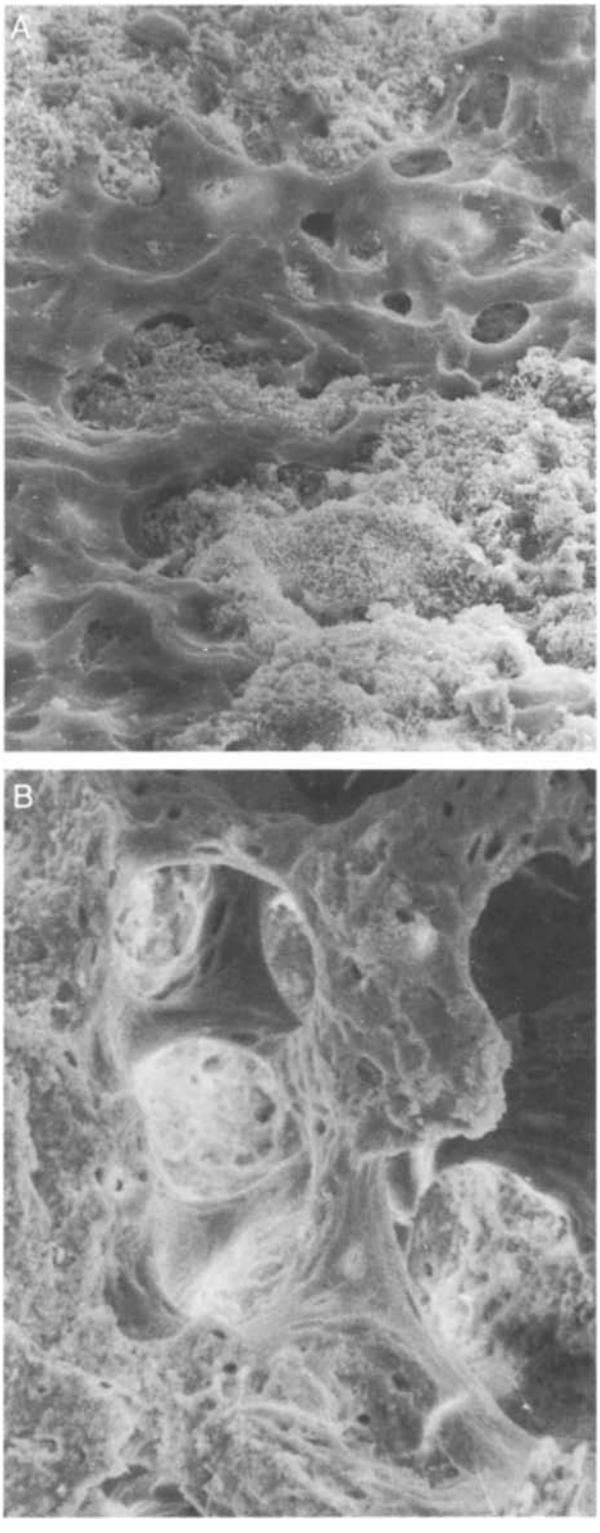

Fig. 7. SEM at day 21 of (A) layer (×800) and (B) trabeculae of newly formed bone (×240) bonding to the surface of MBCP Bm and observed after treatment with sodium hypochlorite.

value of this activity as a reliable marker for osteoclast in culture is discussed [26, 27], and they possess receptors for calcitonin [12, 28]. Recently, specific antibodies were raised against some osteoclast cell surface antigens, and immunohistochemical methods were proposed for osteoclast identification [29–32].

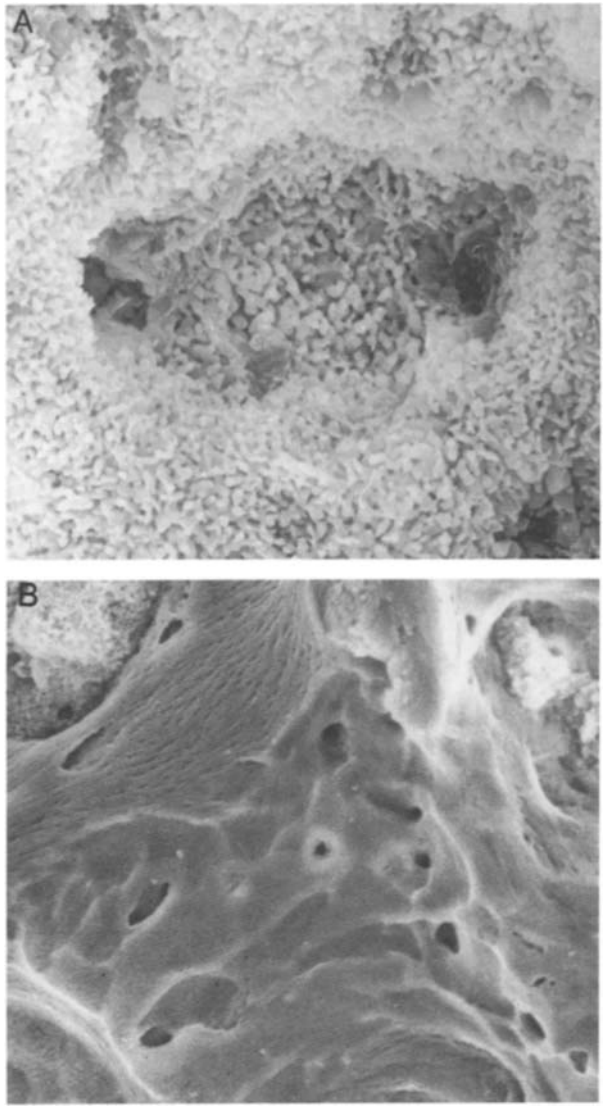

Fig. 8. SEM at day 21, after sodium hypochlorite treatment, of a resorption lacunae found at the surface of (A) Bonap biomaterial (×2300) and (B) newly formed bone (×380) onto Bonap implant.

Giant cells elicited in contact with mineralized bone particles have some morphological features of osteoclasts, such as multinuclearity, but do not show a ruffled border or TRAP activity [9, 17, 33, 34]. Moreover, they break down bone particles by a process resembling phagocytosis.

In our study, implantation in bone of two types of Ca-P macroporous ceramics was followed by osteogenesis inside the implant and by remodeling of the newly formed bone and resorption of the biomaterials. The resorption processes appeared to involve at least two distinct multinucleated cell types. The first type, OLC, observed as soon as day 7 after implantation, includes cells with some features of osteoclasts: multinuclearity, TRAP activity, and ruffled border. These cells were found to be associated with erosion pits at the surface of both biomaterials and newly formed bone. Moreover, TRAP+ activity and increased microporosity were found in the biomaterials underneath these cells suggesting an extracellular dissolution of the biomaterials underneath OLC. However, the ruffled border appeared somewhat different in the cells resorbing the newly formed bone or the biomaterials. A typical ruffled border was observed in the osteoclasts in contact with the newly formed bone. The

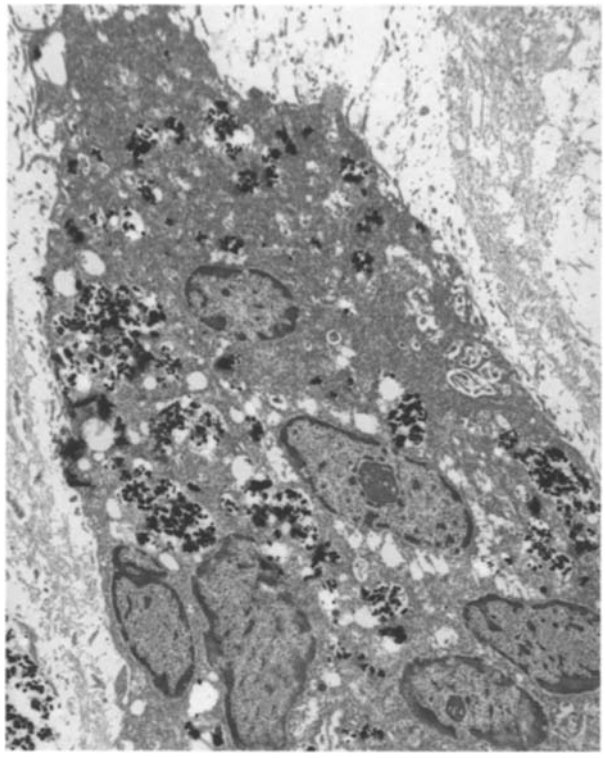

Fig. 9. TEM of a GMNC found, at day 14, at the surface of Bonap Bm. Note the presence of numerous vacuoles with large accumulation of mineral crystals (×3900).

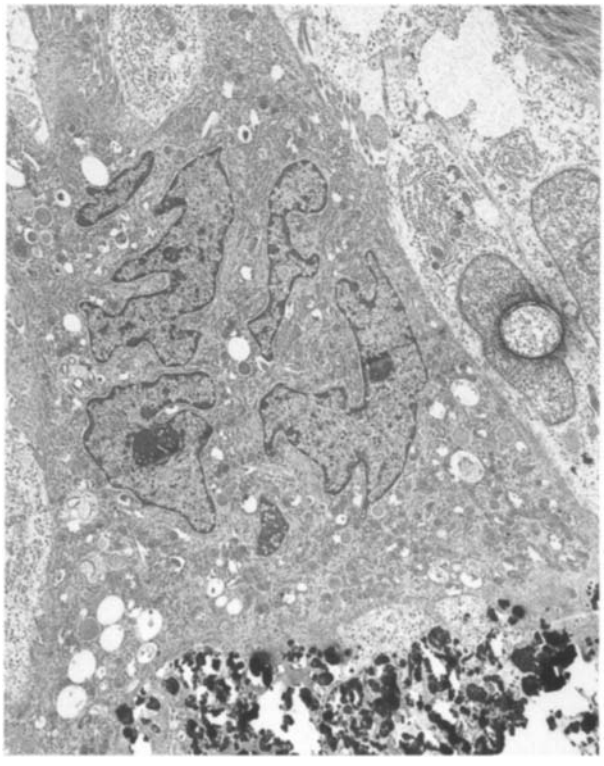

Fig. 10. TEM of an osteoclast-like cell observed at day 14, in contact with the surface of Bonap Bm. Note the absence of mineral crystal inside the cell (×3300).

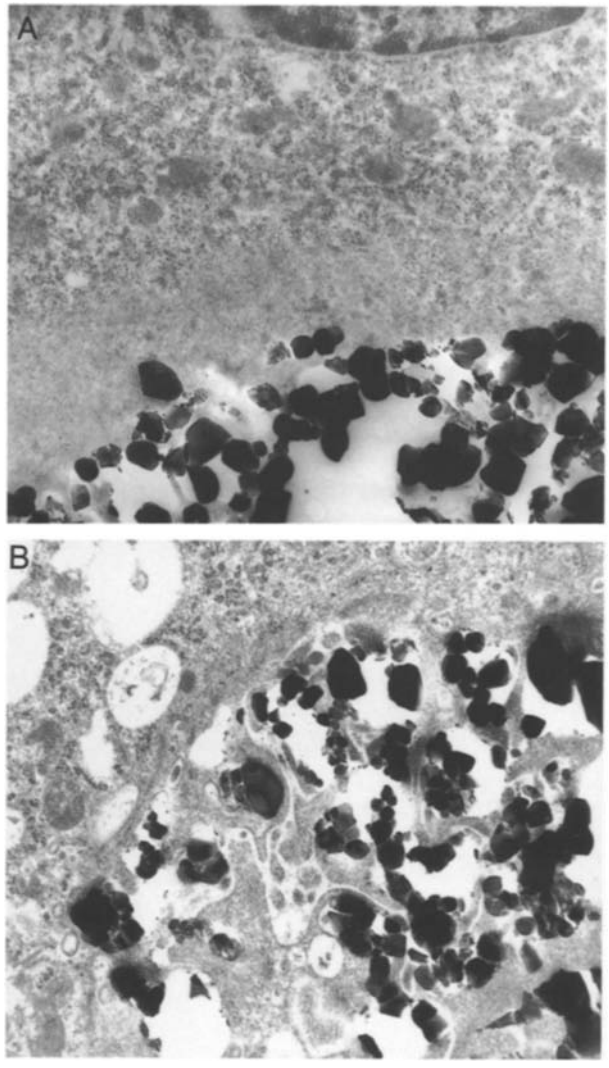

Fig. 11. TEM showing details of the cytoplasmic membrane differentiation of OCL cell found, at day 14, in contact with MBCP Bm. **(A)** Detail of the clear zone (×14,800) and **(B)** detail of the ruffling zone with infoldings inside the microporosity, between mineral crystals (×13,000).

osteoclast-like cells in contact with the biomaterial showed characteristic clear zones and ruffling with infoldings threading between the mineral crystals of the biomaterial. These results suggest that the morphological appearance of the ruffled border depends on the mineralized matrix to be resorbed.

It is usually accepted that osteoclast progenitors are related to mononuclear hematopoietic precursors [10–12, 35]. Thus, osteoclasts or their precursors could migrate, with ingrowth of vascularized connective tissue, from the medullar spaces to the lacunae inside the biomaterials.

The second type of multinucleated cells, GMNC, are huge, containing numerous nuclei and large vacuoles with accumulation of mineral crystals. They show no TRAP activity and develop no ruffled border. They were observed only in contact with the biomaterials and never in relationship with the newly formed bone. Microporosity in the biomaterials under these cells was not significantly increased. These cells were comparable to the giant cells found in the

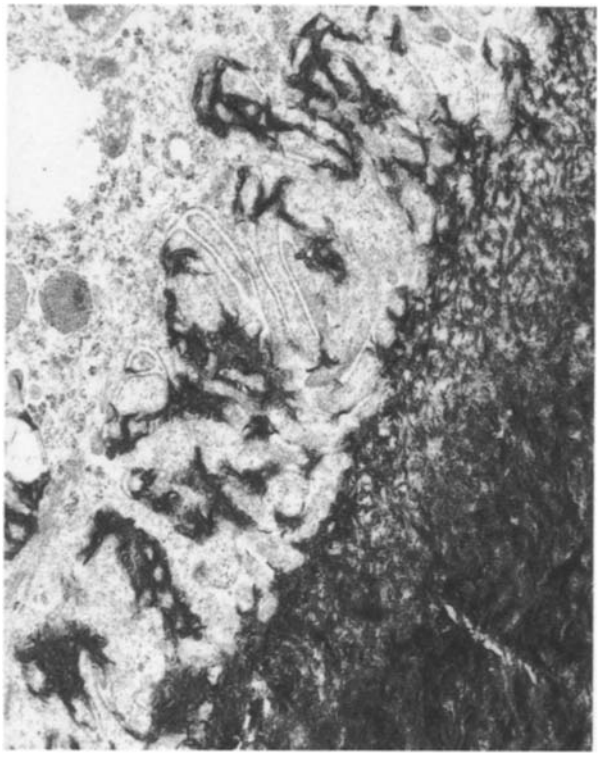

Fig. 12. TEM of the cytoplasmic membrane differentiation in an osteoclast observed, at day 21, in contact with newly formed bone. Note lower mineral density in bone tissue underneath the ruffled border and presence of hydroxyapatite crystals between infoldings (×15,000).

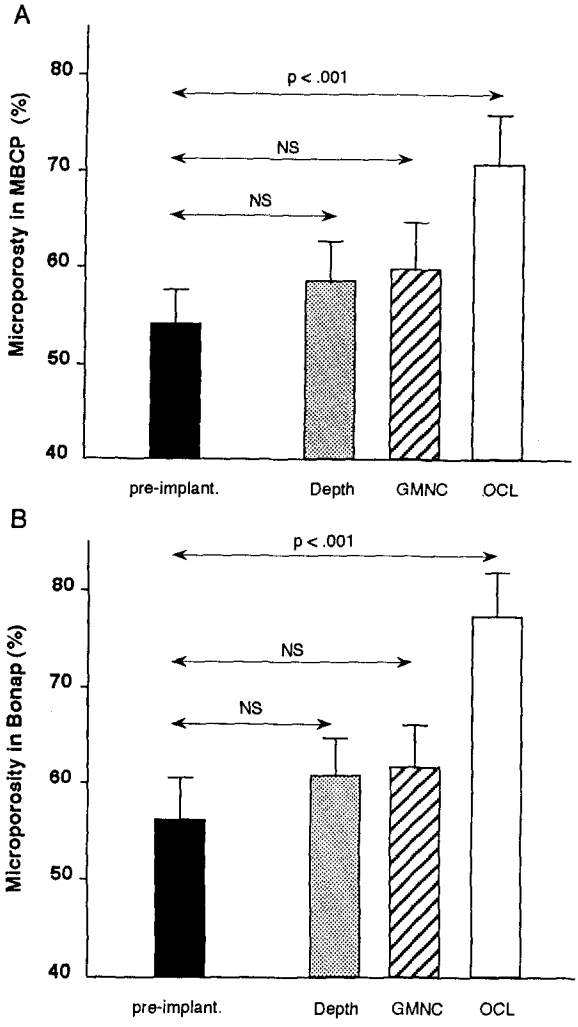

Fig. 13. The microporosity inside (**A**) MBCP and (**B**) Bonap biomaterials was measured before and at day 14 after implantation, in the depth of the biomaterials and in the superficial regions underneath GMNC and OCL. In both biomaterials, the microporosity significantly increased only under OCL cells.

inflammatory tissue of the foreign body reaction. It is usually accepted that they generate by fusion of mature cells of the monocyte/macrophage lineage [15, 16]. However, in our experiment, GMNC were not observed in association with any inflammatory tissue.

Tissue response to implantation of mineralized materials seems to differ according to host species, receiving tissue and chemical composition of the implant, particularly the presence of bone proteins [36]. In this study, the results observed were similar in both types of biomaterials. However, intensity of the response in terms of osteogenesis and number of OCL differed at day 7 and 14 between the two types of biomaterial, but was similar at day 21. Differences in the architectural organization of the materials, particularly in the connections between the macropores, may modify the spreading of the connective tissue and the migration of precursor cells. However, this factor was not studied in this experiment.

Thus, the true role of the implanted material in the cell differentiation is not clear, and controversial results have been reported. When implanted subcutaneously in the rat or onto chorioallantoic membranes of chick embryos [36, 37], devitalized mineralized or demineralized bone particles elicited the recruitment of multinucleated cells. They exhibited some phenotypic features of osteoclasts such as multinuclearity and membrane specializations (clear zones and ruffled borders), TRAP activity, inhibition of resorption by calcitonin, and presence of receptors for this hormone [7, 36–39]. In contrast, multinucleated cells recruited in subcutaneous implants of mineralized bone particles and slices in rabbits showed a TRAP activity considerably weaker than in host osteoclasts, no tartrate-resistant acid ATPase activity, and did not stain with an osteoclast-specific monoclonal antibody [9].

The discrepancy between these studies may be related to host species and/or to differences in the nature or preparation of the implanted mineralized matrix. It was demonstrated that chemical composition of the implanted material influences the degree of osteoclast differentiation. The formation of mineral matrix complexes by the adsorption to hydroxyapatite of bone extract or osteocalcin enhanced ruffled border formation and the presence of specific osteoclast antigen on elicited multinucleated cells [36]. When implanted subcutaneously, synthetic crystalline apatite was reported to generate multinucleated cells showing osteoclastic features, but only when associated with osteocalcin [40].

Osteoblasts synthesize collagenous and noncollagenous proteins of the bone matrix. Among them, osteocalcin was hypothesized to favor differentiation of the ruffled border of the osteoclast [36, 40] and osteopontin to help the binding of this cell to hydroxyapatite [41–43].

Consequently, the resorption events occurring in Ca-P ceramics implanted in bone cannot be dissociated from the

simultaneous bone formation. In our experiment, new bone was observed as early as day 7 after implantation onto the surface of biomaterials. Amount of bone proteins, synthesized by osteoblasts, could circulate with biological fluids in the microporosity of the implant. Thus, the Ca-P ceramics progressively enriched in bone proteins could then favor osteoclastic differentiation. This could explain that the number of OLC resorbing the biomaterials increased from day 7 after implantation in both biomaterials.

From these data we conclude that osteogenesis occurs inside macroporous Ca-P ceramics implanted in bone. Remodeling of the newly formed bone and resorption of the biomaterials appeared to be associated with at least two types of multinucleated cells. Osteoclast-like cells could remodel newly formed bone and resorb the biomaterials progressively enriched in bone proteins, according to an extracellular mechanism, similar to that observed in physiological osteoclastic resorption of bone; giant multinucleated cells could resorb the biomaterials by phagocytosis.

Acknowledgments. The authors particularly wish to thank R. Z. Legeros (College of Dentistry, New York University) for supplying the Bonap biomaterial and J. C. Carbonnier (Zimmer France) for supplying the biphasic calcium phosphate. The authors express their appreciation to N. Thierry and D. Dumont for their assistance with the preparation of this manuscript.

References

1. Jarcho M (1981) Calcium phosphate ceramics as hard tissue prosthetics. Clin Orthop 157:259–278
2. Kenney EB, Lekovic V, Sa Ferreira JC, Han T, Dimitrijevict Carranza FA Jr (1986) Bone formation within porous hydroxyapatite implants in human periodontal defects. J Periodontol 57:76–83
3. Holmes RE, Bucholz RW, Mooney V (1987) Porous hydroxyapatite as a bone graft substitute in diaphyseal defects: a histometric study. Orthop Res 5:114–121
4. Okumura M, Ohgushi H, Tamai S, Shors EC (1991) Primary bone formation in porous hydroxyapatite ceramic: a light and scanning electron microscopic study. Cells Mater 1:29–34
5. Ohgushi H, Goldberg VM, Caplan AI (1989) Heterotopic osteogenesis in porous ceramics induced by marrow cells. J Orthop Res 7:568–578
6. Takeshita N, Akagi T, Yamasaki M, Ozeki T, Nojima T, Hiramatsu Y, Nagai N (1992) Osteoclastic features of multinucleated giant cells responding to synthetic hydroxyapatite implanted in rat jaw bone. J Electron Microsc 41:141–146
7. Glowacki J, Cox KA (1986) Osteoclastic features of cells that resorb bone implants in rats. Calcif Tissue Int 39:97–103
8. Ogilvie A, Frank RM, Benque EP, Gineste M, Heughebaert M, Hemmerle J (1987) The biocompatibility of hydroxyapatite implanted in the human periodontium. J Periodont Res 22:270–283
9. Marks SC, Chambers TJ (1991) The giant cells recruited by subcutaneous implants of mineralized bone particles and slices in rabbits are not osteoclasts. J Bone Miner Res 6:395–400
10. Ash P, Loutit JF, Townsend KMS (1980) Osteoclasts derived from haematopoietic stem cells. Nature 283:669–670
11. Mundy GR, Roodman GD (1987) Osteoclast ontogeny and function. In: Peck WA (ed) Bone and mineral research, Vol 5. Elsevier, Amsterdam, New York, Oxford, pp 209–279
12. Marks SC, Popoff SN (1988) Bone cell biology: the regulation of development, structure and function in the skeleton. Am J Anat 183:1–44
13. Vaes G (1988) Cellular biology and biochemical mechanism of bone resorption: a review of recent developments on the formation, activation, and mode of action of osteoclasts. Clin Orthop 231:239–271
14. Sutton JS, Weiss L (1966) Transformation of monocytes in tissue culture into macrophages, epithelioid cells, and multinucleated giant cells: an electron microscope study. J Cell Biol 28: 303–332
15. Papadimitriou JM, Spector WG (1971) The origin, properties and fate of epithelioid cells. J Pathol 105:187–203
16. Mariano M, Spector WG (1974) The formation and properties of macrophage polykaryon inflammatory giant cells. J Pathol 113: 1–19
17. Holtrop ME, Cox CA, Glowacki J (1982) Cells of the mononuclear phagocytic system resorb implanted bone matrix: a histologic and ultrastructural study. Calcif Tissue Int 34:488–494
18. Chambers TJ, Revell PA, Fuller K, Athanasou NA (1984) Resorption of bone by isolated rabbit osteoclasts. J Cell Sci 66: 383–399
19. Jones SJ, Boyde A (1977) Some morphological observations on osteoclasts. Cell Tissue Res 185:387–397
20. Baron R (1989) Molecular mechanisms of bone resorption by the osteoclast. Anat Rec 224:317–324
21. Baron R, Neff L, Brown W, Courtoy P, Louvard D, Farquhar MG (1988) Polarized secretion of lysosomal enzymes: codistribution of cation-independent mannose-6-phosphate receptors and lysosomal enzymes along the osteoclast exocytic pathway. J Cell Biol 1063:1863–1872
22. Blair HC, Teitelbaum SL, Ghiselli R, Gluck S (1989) Osteoclastic bone resorption by a polarized vacuolar proton pump. Science 245:855–857
23. Arnett TR, Dempster DW (1990) Protons and osteoclasts. J Bone Miner Res 5:1099–1103
24. Minkin C (1982) Bone acid phosphatase: tartrate-resistant acid phosphatase as a marker of osteoclastic function. Calcif Tissue Int 34:285–290
25. Andersson GN, Marks SC (1989) Tartrate-resistant acid ATPase as a cytochemical marker for osteoclasts. J Histochem Cytochem 37:115–117
26. Hattersley G, Chambers TJ (1989) Generation of osteoclastic function in mouse bone marrow cultures: multinuclearity and tartrate-resistant acid phosphatase are unreliable markers for osteoclast differentiation. Endocrinology 124:1689–1696
27. Modderman WE, Tuinenfburg-Bol Raap AC, Nijweide PJ (1991) Tartrate-resistant acid phosphatase is not an exclusive marker for mouse osteoclasts in cell culture. Bone 12:81–87
28. Hattersley G, Chambers TJ (1989) Calcitonin receptors as markers for osteoclastic differentiation: correlation between generation of bone-resorptive cells and cells that express calcitonin receptors in mouse bone marrow cultures. Endocrinology 125: 1606–1612
29. Oursler MJ, Bell LV, Clevinger B, Osdoby P (1985) Identification of osteoclast-specific monoclonal antibodies. J Cell Biol 100:1592–1600
30. Horton MA, Lewis D, McNulty K, Pringle AS, Chambers TJ (1985) Monoclonal antibodies to osteoclastomas (giant cell bone tumors): Definition of osteoclast-specific antigens. Cancer Res 45:5663–5669
31. Chilosi M, Giglioli E, Lestani M, Menestrina F, Fiore-Donati L (1988) Immunohistochemical characterization of osteoclasts and osteoclast-like cells with monoclonal antibody MB1 on paraffin-embedded tissues. J Pathol 156:251–254
32. Kukita T, Roodman GD (1989) Development of a monoclonal antibody to osteoclasts formed in vitro which recognizes mononuclear osteoclast precursors in the marrow. Endocrinology 125:630–637
33. Popoff SN, Marks SC (1986) Ultrastructure of the giant cell infiltrate of subcutaneously implanted bone particles in rats and mice. Am J Anat 177:491–503
34. Kelly J, McNulty JA, Schneider GB (1988) Histochemical and morphological comparison of osteoclasts and multinucleated giant cells recruited to ectopic bone implants. J Cell Biol 37:3376
35. Kerby JA, Hattersley G, Collins DA, Chambers TJ (1992) Derivation of osteoclasts from hematopoietic colony-forming cells in culture. J Bone Miner Res 7:353–362
36. Webber D, Osdoby P, Hauschka P, Krukowski M (1990) Correlation of an osteoclast antigen and ruffled border on giant cells

formed in response to resorbable substrates. J Bone Miner Res 5:401–410
37. Krukowski M, Kahn AJ (1982) Inductive specificity of mineralized bone matrix in ectopic osteoclast differentiation. Calcif Tissue Int 34:474–479
38. Bagi CM, Miller SC (1989) Osteoclast features of cells that resorb demineralized and mineral-containing bone implants in rats. Scanning Microsc 3:963–970
39. Goldring SR, Roelke M, Glowacki J (1988) Multinucleated cells elicited in response to implants of devitalized bone particles possess receptors for calcitonin. J Bone Miner Res 3:117–120
40. Glowacki J, Rey C, Glimcher MJ, Cox K, Lian J (1991) A role for osteocalcin in osteoclast differentiation. J Cell Biochem 45: 292–302
41. Franzen A, Heinegard D (1985) Proteoglycans and bone proteins of rat bone. Purification and biosynthesis of major noncollagenous macromolecules. In: Butler WT (ed) The chemistry and biology of mineralized tissues. Ebsco Media, Birmingham, Alabama, pp 132–141
42. Horton MA (1988) Osteoclast-specific antigens. ISI Atlas of Science. Immunology 1:35–42
43. Reinholt FP, Kultenby K, Oldberg A, Heinegard D (1990) Osteopontin: a possible anchor of osteoclast to bone. Proc Natl Acad Sci USA 87:4473–4475